


## Partial remote synchronization in star-like networks with partial connections among leaf nodes

Zhiyin Yang,<sup>1</sup> Dehua Chen ,<sup>1</sup> Gang Hu,<sup>2</sup> and Zonghua Liu<sup>1,\*</sup>

<sup>1</sup>*School of Physics and Electronic Science, East China Normal University, Shanghai 200241, People's Republic of China*

<sup>2</sup>*Department of Physics, Beijing Normal University, Beijing 100875, People's Republic of China*



(Received 11 August 2023; accepted 30 November 2023; published 15 December 2023)

To understand how the long connections of a brain functional network come from the short connections of its corresponding structural network, remote synchronization (RS) was recently studied in star graph networks. However, the motif of the star graph cannot completely characterize the features of brain networks as the leaf nodes of a star graph may also be connected to each other to some extent in real brain networks. Especially, the dynamics of a star motif in a brain network will be seriously influenced by its surrounding nodes, i.e., other parts of the brain network. To study RS of real brain networks, we here present a model of star-like networks by considering both the partial connections among leaf nodes and the influence of other parts of the brain network. We find that RS will not appear in all leaf nodes and instead appears only in the group of indirectly connected leaf nodes when the frequency difference between the hub and leaf nodes is not large enough, resulting in the concept of *partial RS* (PRS). Further, we find that the partial connections among leaf nodes favor PRS, implying that PRS can more easily appear in real brain networks than RS and thus provides a different way to understand the mechanism of long connections in brain functional networks. Moreover, we find another kind of PRS, i.e., double PRS, and discuss the dependence of PRS on system parameters. Finally, a brief theoretical analysis is provided to explain the results.

DOI: [10.1103/PhysRevResearch.5.043253](https://doi.org/10.1103/PhysRevResearch.5.043253)

### I. INTRODUCTION

The human brain is the most complicated system, and understanding it has been being a challenging problem for a long time. It is well known that the human brain can be characterized by two kinds of networks, i.e., structural and functional networks. The former is obtained from Diffusion Weighted Magnetic Resonance Imaging (DW-MRI) data, in which connections represent axonal fibers [1]. As the cerebral cortex is an optimal network of the trade-off between wiring cost and efficiency, the majority of its anatomical connections are short connections in space [2–4]. The latter is obtained from the Blood Oxygen Level Dependent (BOLD) functional Magnetic Resonance Imaging (fMRI) time series of cortical areas, in which connections represent statistically significant correlations between two time series [5]. It has been revealed that any two cortical areas connected by a functional connection are, in general, spatially separated and there is no edge connecting the two corresponding nodes in the anatomical connectivity network, i.e., long connections in space. Then, a natural question arises: How do the long connections of the functional network emerge from the short connections of the structural network? This question is not trivial because it

might provide meaningful insights about the functional organization of distant neural assemblies during diverse cognitive or pathological states [6].

A possible way to answer this question is through the concept of remote synchronization (RS) proposed by Bergner *et al.* in 2012 [7]. RS occurs when two or more subsystems that are not directly coupled synchronize while the ones between them do not [8,9]. The paradigmatic model of RS is the motif of a star graph where the natural frequency of the central hub is much larger than that of its leaf nodes so that the hub node will not synchronize with the leaf nodes but serves as a transmitter of information to induce synchronization among all the leaf nodes. The study of RS is currently a hot topic in the fields of complex networks and synchronization, and many results have been achieved [10–12]. For example, it was revealed that network symmetries play a central role in RS and the anatomical symmetry of the brain network plays a role in neural synchronization by determining correlated functional modules across distant locations [6,13–15]. Lacerda *et al.* investigated the role of the initial conditions in RS and found the phenomenon of multistability [16]. Kang *et al.* found that there are, indeed, motifs of star graphs in brain networks and the connection of two motifs of star graphs will make RS appear between distant nodes [17]. Cao *et al.* extended the concept of RS to multilayered community networks with star-like topology [18]. Further, it was shown that RS can even be induced by phase frustrations [19–22].

On the other hand, it is well known that a real brain network has both community and rich-club topology and its degree distribution is an approximate power law [23,24]. In this unique network, each node has neighboring nodes and

\*zhliu@phy.ecnu.edu.cn

Published by the American Physical Society under the terms of the [Creative Commons Attribution 4.0 International license](https://creativecommons.org/licenses/by/4.0/). Further distribution of this work must maintain attribution to the author(s) and the published article's title, journal citation, and DOI.

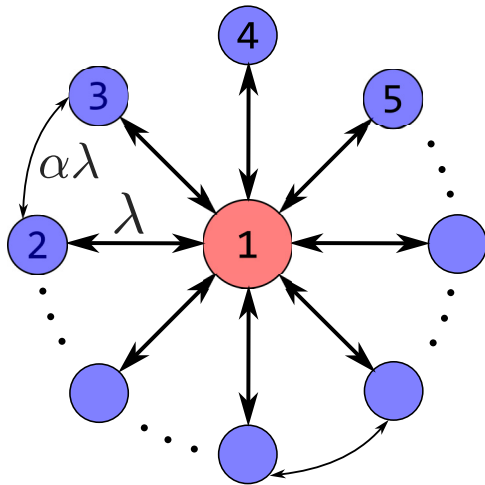


FIG. 1. Schematic illustration of the PRS model of a star-like network with partial connections among the leaf nodes where node 1 represents the central hub node and the others represent the leaf nodes. The coupling strength between the hub and leaf nodes is assumed to be  $\lambda$ , and that among the leaf nodes is assumed to be  $\alpha\lambda$ . The number of connections among leaf nodes can be more than 1.

thus can be approximately considered a motif of a star graph. Thus, understanding the dynamics of the star graph will be of great help to understand how brain functional networks come from their corresponding structural networks. However, in a real brain network, each node and its neighboring nodes will not be a pure motif of a star graph and will be seriously influenced by other parts of the brain network. To consider this characteristic feature, we here present a model of a star-like motif to study RS by considering both the partial connections among the leaf nodes of the star graph and the influence of other parts of the brain network. For convenience, we divide the leaf nodes into two groups. One group is the connected leaf nodes, and the other is the indirectly connected leaf nodes. Interestingly, we find that RS will appear only in the group of indirectly connected leaf nodes and not in all the leaf nodes, which is named *partial RS* (PRS). Further, we show that the partial connections among leaf nodes favor PRS. Moreover, we find another kind of PRS called *double PRS*. Finally, a brief theoretical analysis is provided to explain these results.

## II. A STAR-LIKE NETWORK MODEL OF PARTIAL REMOTE SYNCHRONIZATION WITH PARTIAL CONNECTIONS AMONG LEAF NODES

As mentioned above, our model will consider two aspects, i.e., partial connections among the leaf nodes of a star graph and the influence of other parts of the brain network, in contrast to previous RS models that mainly focused on the networks of the star graph. For convenience, we let the influence from other parts of the brain network be merged into the partial connections among the leaf nodes. Figure 1 shows a schematic illustration of the PRS model of a star-like network where the central node 1 represents the hub node, nodes 2 to  $N$  represent the leaf nodes, and the couplings are considered bidirectional, with  $N$  being the total number of nodes. The

characteristic feature of Fig. 1 is the connections between the leaf nodes such as that between nodes 2 and 3, in contrast to previous RS models of a pure star graph. Considering the fact that the connections among leaf nodes may come either from themselves or from other parts of the brain network, for simplicity, we let their coupling strength be different from that between the hub and leaf nodes. That is, we let the coupling strength between any two connected leaf nodes be  $\alpha\lambda$ , where  $\lambda$  represents the coupling strength between the hub and leaf nodes. Figure 1 will go back to previous RS models of the star graph when  $\alpha = 0$ .

To study the RS in Fig. 1, we let the nodes' dynamics be the Stuart-Landau oscillator [7], and thus, the network's dynamics can be represented by the coupled Stuart-Landau oscillators as follows:

$$\begin{aligned} \dot{z}_h &= (\gamma + i\omega_h - |z_h|^2)z_h + \frac{\lambda}{k_h} \sum_{\ell=2}^N (z_\ell - z_h), \\ \dot{z}_\ell &= (\gamma + i\omega_\ell - |z_\ell|^2)z_\ell + \frac{\lambda}{k_\ell} (z_h - z_\ell) \\ &\quad + \frac{\alpha\lambda}{k_\ell} \sum_{\ell'=2}^N \delta(\ell, \ell') (z_{\ell'} - z_\ell), \end{aligned} \tag{1}$$

where  $h$  and  $\ell$  represent the hub and leaf nodes, respectively, with  $h = 1$  and  $\ell = 2, \dots, N$ .  $\omega_h$  and  $\omega_\ell$  are the natural angular frequencies of the hub and leaf nodes, respectively.  $k_h$  and  $k_\ell$  represent the degrees of the hub and leaf nodes, respectively, with  $k_h = N - 1$ .  $\delta(\ell, \ell')$  represents the connection between two leaf nodes, with  $\delta(\ell, \ell') = 1$  if the leaf nodes  $\ell$  and  $\ell'$  are connected and  $\delta(\ell, \ell') = 0$  otherwise.  $\gamma$  is a parameter representing the nondimensional distance from the Hopf bifurcation onset. For an isolated oscillator, the stationary solution  $z = 0$  is stable for  $\gamma < 0$ ; in contrast, when  $\gamma > 0$ ,  $z$  oscillates in a limit cycle, and  $\sqrt{\gamma}$  is the amplitude of  $|z|$ . In this work, we let  $\gamma = 1$ .

In Eq. (1),  $z_h$  and  $z_\ell$  are complex variables and can be represented as  $z_h = r_h e^{i\theta_h}$  and  $z_\ell = r_\ell e^{i\theta_\ell}$ , with  $r_h$  and  $r_\ell$  and  $\theta_h$  and  $\theta_\ell$  being their amplitudes and phase angles, respectively. Then, Eq. (1) can be rewritten in the polar coordinate system as

$$\begin{aligned} \dot{r}_h &= \gamma r_h - r_h^3 + \frac{\lambda}{k_h} \sum_{\ell=2}^N [r_\ell \cos(\theta_\ell - \theta_h) - r_h], \\ \dot{\theta}_h &= \omega_h + \frac{\lambda}{k_h} \sum_{\ell=2}^N \frac{r_\ell}{r_h} \sin(\theta_\ell - \theta_h), \\ \dot{r}_\ell &= \gamma r_\ell - r_\ell^3 + \frac{\lambda}{k_\ell} [r_h \cos(\theta_h - \theta_\ell) - r_\ell] \\ &\quad + \frac{\alpha\lambda}{k_\ell} \sum_{\ell'=2}^N \delta(\ell, \ell') [r_{\ell'} \cos(\theta_{\ell'} - \theta_\ell) - r_\ell], \\ \dot{\theta}_\ell &= \omega_\ell + \frac{\lambda}{k_\ell} \frac{r_h}{r_\ell} \sin(\theta_h - \theta_\ell) \\ &\quad + \frac{\alpha\lambda}{k_\ell} \sum_{\ell'=2}^N \delta(\ell, \ell') \frac{r_{\ell'}}{r_\ell} \sin(\theta_{\ell'} - \theta_\ell). \end{aligned} \tag{2}$$

Our numerical simulations in the next section will be based on Eq. (2).

We notice from Fig. 1 that the leaf nodes can be divided into two groups, i.e., the connected group and the indirectly connected group. In general, the connected group will be easier to synchronize than the indirectly connected group, and thus, the behaviors of the two groups will be different. Considering the fact that the phase synchronization between two oscillators implies a constant or bounded phase difference, we suggest that the phase synchronization of the two groups should be measured by different quantities because their phase differences may be different constants. In detail, we follow Ref. [7] and introduce an order parameter to measure the phase synchronization between two leaf oscillators, defined as

$$r_{\ell\ell'} = \left| \lim_{T \rightarrow \infty} \frac{1}{T} \int_t^{t+T} e^{i[\theta_\ell(t) - \theta_{\ell'}(t)]} dt \right|, \quad (3)$$

where  $T$  is the time window to measure the correlation. Then, the order parameter  $R$  of all the leaf nodes can be given as

$$R_{\ell\ell} = \frac{2}{(N-1)(N-2)} \sum_{\ell=2, \ell' > \ell}^N r_{\ell\ell'}, \quad (4)$$

where  $r_{\ell\ell'}$  runs over all pairs of the leaf nodes. Similarly, we introduce an order parameter to measure the phase synchronization between the hub and a leaf oscillator, defined as

$$r_{h\ell'} = \left| \lim_{T \rightarrow \infty} \frac{1}{T} \int_t^{t+T} e^{i[\theta_h(t) - \theta_{\ell'}(t)]} dt \right|. \quad (5)$$

Then, the order parameter  $R$  for the connections between the hub and all the leaf nodes can be given as

$$R_{h\ell} = \frac{1}{N-1} \sum_{\ell'=2}^N r_{h\ell'}, \quad (6)$$

where  $r_{h\ell'}$  runs over all the links between the hub and leaf nodes.  $R$  will be between 0 and 1, and a larger value of  $R$  represents a stronger phase synchronization. According to Ref. [7], the system will be remotely synchronized when the value of  $R_{\ell\ell}$  is approximately unity while the value of  $R_{h\ell}$  is smaller than unity, i.e., the coexistence of synchronization between the indirectly connected leaf nodes and nonsynchronization between the directly connected leaf and hub nodes.

Further, we let  $N_I$  and  $N_{II}$  be the numbers of the connected and indirectly connected leaf nodes, respectively, with  $N_I + N_{II} = N - 1$ . The order parameter  $R$  for the group of connected leaf nodes can be given as

$$R_{\ell\ell}^c = \frac{1}{\sum_{\ell, \ell'=1}^{N_I} \delta(\ell, \ell')} \sum_{\ell, \ell'=1}^{N_I} \delta(\ell, \ell') r_{\ell\ell'}, \quad (7)$$

where  $r_{\ell\ell'}$  runs over all pairs of the connected leaf nodes. We define  $\delta(\ell, \ell') = 1$  if the leaf nodes  $\ell$  and  $\ell'$  are connected and  $\delta(\ell, \ell') = 0$  otherwise. Similarly, the order parameter  $R$  for the group of indirectly connected leaf nodes can be given as

$$R_{\ell\ell}^i = \frac{2}{N_{II}(N_{II}-1)} \sum_{\ell=1, \ell' > \ell}^{N_{II}} r_{\ell\ell'}, \quad (8)$$

where  $r_{\ell\ell'}$  runs over all pairs of the indirectly connected leaf nodes. The order parameter  $R$  for the connections between the hub and the connected leaf nodes can be given as

$$R_{h\ell}^c = \frac{1}{N_I} \sum_{\ell'=1}^{N_I} r_{h\ell'}, \quad (9)$$

where  $r_{h\ell'}$  runs over all the connections between the hub and the connected leaf nodes. Similarly, the order parameter  $R$  for the connections between the hub and the indirectly connected leaf nodes can be given as

$$R_{h\ell}^i = \frac{1}{N_{II}} \sum_{\ell'=1}^{N_{II}} r_{h\ell'}, \quad (10)$$

where  $r_{h\ell'}$  runs over all the connections between the hub and the indirectly connected leaf nodes.

### III. PARTIAL REMOTE SYNCHRONIZATION

We now use the formulas in Eqs. (4)–(10) to discuss RS of Eq. (2). For convenience, we let the natural frequency of the hub be fixed at  $\omega_h = 1.5$  and let that of the leaf nodes be  $\omega_\ell = 1.0 + \epsilon_\ell$  for  $\ell = 2, \dots, N$  if not indicated otherwise, with  $\epsilon_\ell$  being small values chosen randomly from a uniform distribution around zero. In this case,  $\epsilon_\ell$  will not significantly influence the difference between the hub and leaf nodes and will make the leaf nodes nonidentical. Let  $\Delta\omega = \omega_h - \langle\omega_\ell\rangle$  be the difference between the natural frequency of the hub and the mean frequency of the leaf nodes. Thus, we have  $\Delta\omega \approx 0.5$ .

#### A. Case with $N = 5$

To discuss RS in Eq. (2) in detail, we take the case with  $N = 5$  as an example. In this case, the randomly chosen natural frequencies are  $\omega_h = 1.5$  and  $\omega_\ell = (1.002, 0.986, 0.991, 1.017)$  for  $\ell = 2, \dots, 5$ . First, we consider the case with  $\alpha = 0$ , which returns back to the motif of a star graph. According to the results of Ref. [7], the chosen  $\Delta\omega \approx 0.5$  is not large enough to induce RS. Figure 2(a) shows the numerical results, where the inset is the network configuration and the red and blue lines represent the dependence of  $R_{h\ell}$  and  $R_{\ell\ell}$  on the coupling strength  $\lambda$ , respectively. We see that the two lines reach  $R = 1$  at the same  $\lambda$ , confirming that there is no RS.

Then, we move to the case with  $\alpha > 0$ , corresponding to the connection between leaf nodes 2 and 3 in Fig. 1. As an example, we consider the case with  $\alpha = 1$ . Figure 2(b) shows the results, where the inset is the network configuration and the red and blue lines represent the dependence of  $R_{h\ell}$  and  $R_{\ell\ell}$  on the coupling strength  $\lambda$ , respectively. We see that similar to Fig. 2(a), the two lines in Fig. 2(b) also reach  $R = 1$  at the same  $\lambda$ , indicating no RS. Is this true? To go deeper to study the influence of the connection between leaf nodes 2 and 3 on RS, we calculate the order parameters for both the group of connected leaf nodes and the indirectly connected group, i.e., the values of  $R_{h\ell}^c$ ,  $R_{\ell\ell}^c$ ,  $R_{h\ell}^i$ , and  $R_{\ell\ell}^i$  for the case with  $\alpha = 1$ . Figure 2(c) shows the results for the group of connected leaf nodes, where the inset gives the network configuration and the red and blue lines represent the dependence of  $R_{h\ell}^c$  and  $R_{\ell\ell}^c$  on

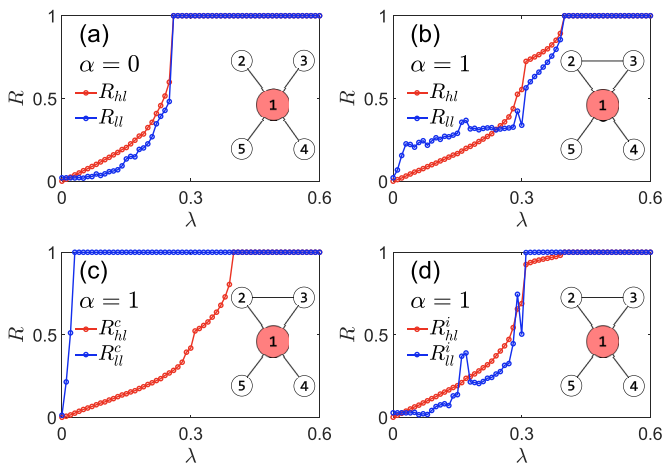


FIG. 2. Partial RS induced by the connection between leaf nodes 2 and 3, with  $N = 5$ ,  $\omega_h = 1.5$ , and  $\omega_\ell = (0.980, 1.005, 0.997, 1.017)$  for  $\ell = 2, \dots, 5$ , where the insets show their network configurations. (a) and (b) show the cases of  $\alpha = 0$  and 1.0, respectively, where the red and blue lines represent the dependence of  $R_{h\ell}$  and  $R_{\ell\ell}$  on the coupling strength  $\lambda$ , respectively. (c) shows the group of connected leaf nodes with  $\alpha = 1$ , where the red and blue lines represent the dependence of  $R_{h\ell}^c$  and  $R_{\ell\ell}^c$  on the coupling strength  $\lambda$ , respectively. (d) shows the group of indirectly connected leaf nodes with  $\alpha = 1$ , where the red and blue lines represent the dependence of  $R_{h\ell}^i$  and  $R_{\ell\ell}^i$  on the coupling strength  $\lambda$ , respectively.

the coupling strength  $\lambda$ , respectively. We see that  $R_{\ell\ell}^c$  reaches unity at a small  $\lambda$ , while  $R_{h\ell}^c$  reaches unity at  $\lambda \approx 0.4$ . That is, the order parameter  $R_{h\ell}^c$  for the connected hub and leaf nodes reaches an unsynchronized state, while the order parameter  $R_{\ell\ell}^c$  for the connected leaf nodes reaches a synchronized state before  $\lambda \approx 0.4$ , indicating a typical RS. Similarly, Fig. 2(d) shows the results for the group of indirectly connected leaf nodes, where the inset gives the network configuration and the red and blue lines represent the dependence of  $R_{h\ell}^i$  and  $R_{\ell\ell}^i$  on the coupling strength  $\lambda$ , respectively. We see that  $R_{\ell\ell}^i$  also reaches unity earlier than  $R_{h\ell}^i$ , confirming the existence of RS again. In conclusion, we find a phenomenon in which the two groups of connected and indirectly connected leaf nodes will show RS independently but not when they are considered as a whole. As the group of connected leaf nodes is not exactly consistent with the definition of RS in Ref. [7], we will not pay attention to it. In the following, we will focus on only the group of indirectly connected leaf nodes because it is exactly consistent with the definition of RS in Ref. [7]. Considering the fact that the group of indirectly connected leaf nodes is only one part of all the leaf nodes, we call its RS *partial RS*.

The PRS in Fig. 2(d) is based on a specific set of  $\omega_\ell$ . Is this PRS robust to other sets of  $\omega_\ell$ ? To answer this question, we carried out extensive numerical simulations and confirmed this result. We find that it is very easy for the two connected leaf nodes, 2 and 3, to be synchronized but the synchronization of the indirectly connected leaf nodes, 4 and 5, is a little complicated. Thus, we will mainly focus on the group of indirectly connected leaf nodes, i.e., the case in Fig. 2(d). Figures 3(a) and 3(b) show two more typical cases with  $\alpha = 1.0$ , where the set of  $\omega_\ell$  is taken as  $\omega_\ell = (0.999, 0.980, 1.012, 1.014)$  in

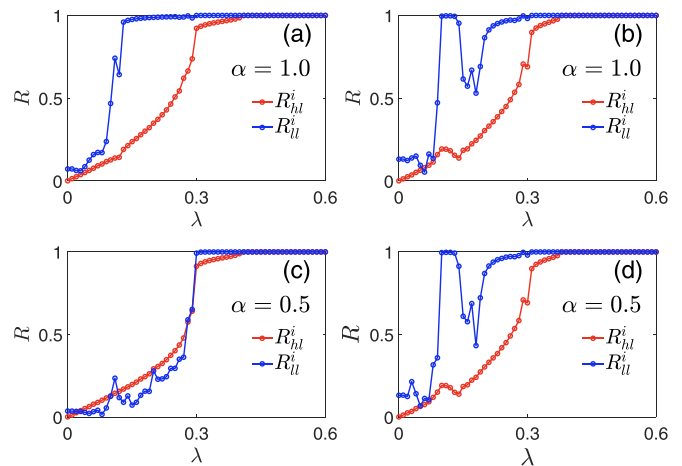


FIG. 3. Double PRS induced by the connection between leaf nodes 2 and 3, with  $N = 5$  and  $\omega_h = 1.5$ , where the red and blue lines represent the dependence of  $R_{h\ell}^i$  and  $R_{\ell\ell}^i$  on the coupling strength  $\lambda$ , respectively. (a) and (b) show the case of  $\alpha = 1.0$ , with  $\omega_\ell = (0.999, 0.980, 1.012, 1.014)$  and  $\omega_\ell = (0.996, 1.018, 0.995, 0.998)$ , respectively. (c) and (d) show the case of  $\alpha = 0.5$ , with  $\omega_\ell = (0.985, 0.996, 1.001, 1.019)$  and  $\omega_\ell = (0.996, 1.018, 0.995, 0.998)$ , respectively.

Fig. 3(a) and  $\omega_\ell = (0.996, 1.018, 0.995, 0.998)$  in Fig. 3(b). We see that Fig. 3(a) is similar to Fig. 2(d), confirming PRS. However, Fig. 3(b) shows another kind of PRS in which there are two separated regions of PRS, i.e., one around  $\lambda = 0.1$  and another around  $\lambda = 0.3$ . We will call this *double PRS*. Correspondingly, we will call the PRS in Fig. 3(a) *single PRS*. That is, we now have two kinds of PRS, i.e., single and double PRS.

We have found phenomena similar to those in Figs. 3(a) and 3(b) for cases with other  $\alpha$ , indicating that they are general for the network in Fig. 1. As an example, Figs. 3(c) and 3(d) show the results for  $\alpha = 0.5$ , with  $\omega_\ell = (0.985, 0.996, 1.001, 1.019)$  in Fig. 3(c) and  $\omega_\ell = (0.996, 1.018, 0.995, 0.998)$  in Fig. 3(d). We see single PRS in Fig. 3(c) but double PRS in Fig. 3(d).

Further, we find that the state of single or double PRS is sensitively dependent on both the set of  $\omega_\ell$  and the connections among leaf nodes. For example, for a fixed set of  $\omega_\ell$ , the state of the system will change between single and double PRS when the connection between leaf nodes 2 and 3 is changed to other nodes such as between leaf nodes 3 and 4 or between leaf nodes 4 and 5. However, for a fixed connection between leaf nodes 2 and 3, the state of the system will also change between single and double PRS for different sets of  $\omega_\ell$ . Figure 4 shows a phase diagram of PRS on  $\omega_4$  and  $\omega_5$  for fixed  $\omega_2 = 0.98$  and  $\omega_3 = 1.02$ , where the blue, yellow, and green regions represent single PRS, double PRS, and no PRS, respectively. We see that the three regions are not smoothly separated from each other and look like a fractal, confirming the sensitivity of PRS to system parameters.

### B. Case with $N = 9$

All the above results were obtained for the fixed network size of  $N = 5$ . To study the influence of network size, we



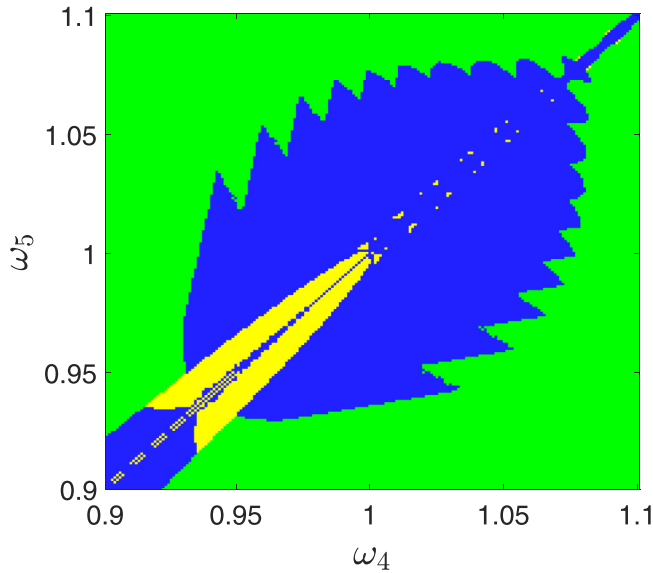


FIG. 4. Phase diagram of PRS on  $\omega_4$  and  $\omega_5$  with fixed  $\omega_2 = 0.98$  and  $\omega_3 = 1.02$ , where the blue, yellow, and green regions represent the single PRS, double PRS, and no PRS, respectively.

gradually increase the number of leaf nodes but leave the hub node unchanged. In this situation, more connections can be added among the leaf nodes, and thus, more configurations of the network can be generated. We find that PRS can still be observed and the areas of PRS increase with the number of connections among the leaf nodes. Figure 5 shows such an example with  $N = 9$  where  $\alpha = 1$  and the natural frequencies are taken as  $\omega_h = 1.5$  and  $\omega_\ell = (0.998, 1.014, 0.981, 0.992, 0.982, 1.004, 0.996, 1.013)$  for  $\ell = 2, \dots, 9$ . The connections among the leaf nodes in Figs. 5(a)–5(f) are gradually increased from 0 to 5. That is, Fig. 5(a) is, in fact, the motif of the star graph with no connections among the leaf nodes. We see that it has no RS and thus confirms the result in Fig. 2(a). However, we see from Fig. 5(b), which has one connection among the leaf nodes, that the blue line for  $R_{\ell\ell}^i$  will reach unity at about  $\lambda = 0.3$ , while the red line for  $R_{h\ell}^i$  is still slightly smaller than unity, indicating the emergence of PRS. We interestingly find that in the coupling range of PRS, the difference between  $R_{\ell\ell}^i$  and  $R_{h\ell}^i$  will become larger and larger as the number of connections among the leaf nodes continues to increase [see Figs. 5(c)–5(f)].

On the other hand, we notice that all the plots in Figs. 5(b)–5(f) show the single PRS but no double PRS. To figure out the reason, we carried out extensive numerical simulations and found that the fixed set of frequencies  $\omega_h$  and  $\omega_\ell$  in Figs. 5(b)–5(f) are the main reason. In fact, it is possible to observe the double PRS if we change the set of frequencies, indicating that both the single and double PRS can be observed in the case with  $N = 9$ .

In addition to the size effect of the network, another key element that influences PRS is the frequency difference between the hub and leaf nodes. To illustrate this, we here fix a set of natural frequencies of leaf nodes  $\omega_\ell$  for  $\ell = 2, \dots, N$  and let the frequency of the hub node  $\omega_h$  gradually increase from 1.0 to a larger value. Then, we check

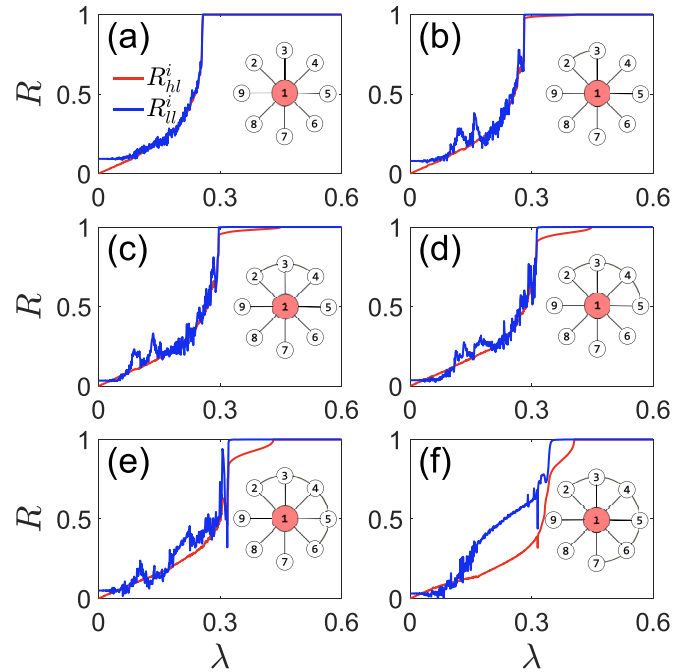


FIG. 5. PRS of the star-like networks with  $N = 9$ , where the natural frequencies are taken as  $\omega_h = 1.5$  and  $\omega_\ell = (0.998, 1.014, 0.981, 0.992, 0.982, 1.004, 0.996, 1.013)$  for  $\ell = 2, \dots, 9$ . (a)–(f) show cases with different network configurations where the connections among the leaf nodes are gradually increased from 0 to 5, respectively. The inset of each panel gives the configuration of the network.

the range of PRS, regardless of whether it is single or double PRS. That is, we measure the value of  $\Delta R \equiv R_{\ell\ell}^i - R_{h\ell}^i$ , provided that  $R_{\ell\ell}^i$  reaches unity. Figures 6(a) and 6(b) show the phase diagrams of  $\Delta R$  on the parameter plane  $(\Delta\omega, \lambda)$  for  $N = 5$  and 9, respectively, with  $\Delta\omega \equiv \omega_h - \omega_\ell$ , where the color bar represents the value of  $\Delta R$  and the sets of natural frequencies of the leaf nodes are fixed at  $\omega_\ell = (0.996, 1.018, 0.995, 0.998)$  in Fig. 6(a) and  $\omega_\ell = (0.989, 1.016, 1.012, 1.010, 1.011, 0.985, 0.989, 0.995)$  in Fig. 6(b). We see from Fig. 6(a) that double PRS occurs for  $0.23 < \Delta\omega < 1.09$  and single PRS occurs for  $\Delta\omega > 1.09$ . Figure 6(b) shows behavior similar to that in Fig. 6(a). In contrast to Figs. 6(a) and 6(b), Figs. 6(c) and 6(d) show the phase diagrams of another set of natural frequencies of leaf nodes for  $N = 5$  and 9, respectively, in which the set of natural frequencies of leaf nodes are fixed at  $\omega_\ell = (0.975, 0.991, 1.008, 1.024)$  in Fig. 6(c) and  $\omega_\ell = (0.981, 0.982, 0.992, 0.996, 0.998, 1.004, 1.013, 1.014)$  in Fig. 6(d). We see that  $\Delta R$  also depends on  $\Delta\omega$  and  $\lambda$ . Therefore, the frequency difference between the hub and leaf nodes has a serious influence on PRS.

#### IV. A BRIEF THEORETICAL ANALYSIS

In the above numerical simulations, we observed three main results: (i) The group of connected leaf nodes will be easily synchronized at a small coupling strength [see Fig. 2(c)]. (ii) The group of indirectly connected leaf nodes will show PRS at a smaller  $\Delta\omega$  where RS is not available for

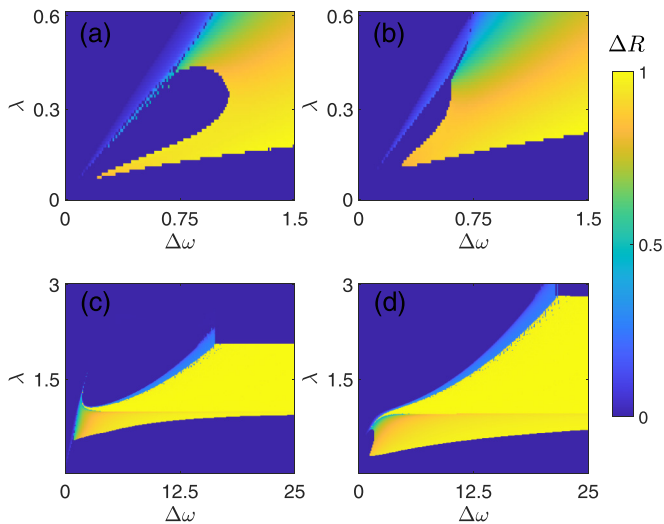


FIG. 6. Phase diagrams of  $\Delta R$  on the parameter plane  $(\Delta\omega, \lambda)$ , where the color bar represents the value of  $\Delta R$ . (a) and (c) show the case with  $N = 5$ , and its network configuration is the same as in Fig. 2(d); (b) and (d) show the case with  $N = 9$ , and its network configuration is the same as in Fig. 5(e). The set of natural frequencies of leaf nodes is fixed as  $\omega_\ell = (0.996, 1.018, 0.995, 0.998)$  in (a),  $\omega_\ell = (0.989, 1.016, 1.012, 1.010, 1.011, 0.985, 0.989, 0.995)$  in (b),  $\omega_\ell = (0.975, 0.991, 1.008, 1.024)$  in (c), and  $\omega_\ell = (0.981, 0.982, 0.992, 0.996, 0.998, 1.004, 1.013, 1.014)$  in (d).

the case of no connections among the leaf nodes [see Fig. 2(a) for no RS and Fig. 2(d) for PRS]. (iii) PRS can be either single or double PRS, depending on the frequency distribution of the leaf nodes (see Fig. 3). To understand the mechanism of these results, we take the case with  $N = 5$  as an example to undertake a theoretical analysis, while the cases with  $N > 5$  can be similarly analyzed.

First, we discuss result (i), i.e., the synchronization in Fig. 2(c). In this case, the influence of the hub node on the two connected leaf nodes can be considered a common perturbation. Thus, the dynamics of the two connected leaf nodes, 2 and 3, can be simplified to

$$\begin{aligned} \dot{z}_2 &= (\gamma + i\omega_2 - |z_2|^2)z_2 + \frac{\alpha\lambda}{2}(z_3 - z_2) + \xi(t), \\ \dot{z}_3 &= (\gamma + i\omega_3 - |z_3|^2)z_3 + \frac{\alpha\lambda}{2}(z_2 - z_3) + \xi(t), \end{aligned} \quad (11)$$

where  $\xi(t)$  represents the perturbation from the hub node. Equation (11) is a typical system of two coupled oscillators when  $\xi(t)$  is ignored. In this case, the coupling term will easily make the largest transverse Lyapunov exponent of two identical or nearly identical oscillators be negative and thus will make the system be synchronized [25,26]. When  $\xi(t)$  is uncorrelated to the dynamics of the system, it can be considered to be a noise common to both  $z_2$  and  $z_3$ . In this case, it is well known that a common noise is helpful for synchronization, called *noise-induced synchronization* [27,28]. Therefore, both the coupling and common noise are helpful for the synchronization in Eq. (11), which results in the early synchronization between connected oscillators 2 and 3 in Fig. 2(c).

Next, we discuss result (ii), i.e., PRS in Fig. 2(d). In this case, we focus on the coupling range in which the two con-

nected leaf nodes are synchronized and thus have stronger influence on the indirectly connected leaf nodes through the hub node. To figure out the mechanism of result (ii), we divide the influence of the network on the two indirectly connected leaf nodes, 4 and 5, into two parts: one directly from the hub's dynamics,  $\xi(t)$ , and one from connected leaf nodes 2 and 3,  $y(t)$ . Thus, the dynamics of the two indirectly connected leaf nodes, 4 and 5, can be simplified to

$$\begin{aligned} \dot{z}_4 &= (\gamma + i\omega_4 - |z_4|^2)z_4 + y(t) + \xi(t), \\ \dot{z}_5 &= (\gamma + i\omega_5 - |z_5|^2)z_5 + y(t) + \xi(t). \end{aligned} \quad (12)$$

As the difference between  $\omega_h$  and  $\omega_\ell$  is relatively large, the hub node will not synchronize with the leaf nodes in the region of PRS. When  $y(t)$  does not exist, the hub node will take only the role of transmitter to make the indirectly connected leaf nodes synchronized, provided that the frequency difference  $\Delta\omega$  is large enough, such as  $\Delta\omega = 1.5$  in Refs. [7,19]. Otherwise, the hub node not may be completely uncorrelated with the leaf nodes when  $\Delta\omega$  is not large enough, such as  $\Delta\omega = 0.5$  in Fig. 2(a). In this case,  $\xi(t)$  cannot be considered a pure transmitter and thus weakens the indirect coupling between nodes 4 and 5, resulting in no RS in Fig. 2(a). However, when  $y(t)$  is considered, it will seriously influence the dynamics of the two indirectly connected leaf nodes, 4 and 5, as its natural frequency is very close to that of nodes 4 and 5. In this sense,  $y(t)$  will behave as a common driving signal to induce a synchronization between nodes 4 and 5 [25,26] and thus result in the observed PRS in Fig. 2(d).

Finally, we discuss result (iii), i.e., double PRS in Fig. 3(d). We notice from Fig. 4 that the areas of double PRS are located around the diagonal line of  $\omega_4 \approx \omega_5$ , indicating that a small difference between  $\omega_4$  and  $\omega_5$  is a necessary condition of double PRS. Based on this condition of  $\omega_4 \approx \omega_5$ , it is possible for the first PRS to appear at a relatively smaller coupling strength  $\lambda$  if the initial conditions of the system are appropriately chosen (see the jumping behaviors in Fig. 3(d) at  $\lambda \approx 0.1$ ). However, this synchronization between indirectly connected nodes 4 and 5 will be broken when the coupling strength  $\lambda$  is further increased. In this case, the further increased coupling actually amplifies the small difference between nodes 4 and 5 and thus induces dynamical instability, similar to the mechanism of the first loop of the double explosive transition in Ref. [29]. The mechanism of the second PRS in Fig. 3(d) is the same as that of the single PRS in Fig. 3(c).

This double PRS may be related to the echo effect involved in cognitive processes. Take epileptic seizures as an example. During the seizure process, the coupling between brain areas will change with time [30], and a patient will undergo four phases: the interictal period, the onset of the seizure, and the propagation and termination phases. Recently, Shen and Liu studied the mechanism of the echo effect [31]. They showed that the echo effect is, in fact, double or multiple coupling ranges of synchronization and can be observed in Electroencephalography (EEG) databases for pediatric subjects with intractable seizures [32] and the resting-state EEG from a long sustained attention task [33]. In this sense, double PRS may provide new insight into the understanding of the echo effect.

## V. DISCUSSION AND CONCLUSIONS

RS is currently a hot topic in the field of complex networks. So far, most efforts have been made for star graphs with various oscillators and frustrations. However, pure star graphs are very rare in realistic systems, and instead, most of them feature star-like graphs, such as brain and social networks. Based on this observation, we here presented a model of star-like graphs in which the leaf nodes were divided into two groups, with one group being weakly connected and the other being unconnected. We found that its RS cannot be described by the previous definition, i.e., all the leaf nodes should be synchronized. Therefore, we extended the concept of RS to PRS, in which only the unconnected leaf nodes are synchronized. This concept of PRS can be conveniently used for realistic cases. For example, in a functional brain network, a connection is considered by asking only whether two remote nodes are synchronized but not whether all the neighboring nodes are synchronized. Appendix A shows evidence from resting-state functional connectivity [34,35].

At the same time, we revealed that the required frequency difference between the hub and leaf nodes for PRS in Fig. 6(a) ( $\Delta\omega \approx 0.23$ ) is much smaller than that for RS in Ref. [7] ( $\Delta\omega \approx 1.5$ ). This finding is practically useful because the frequency differences of neurons in the human brain are usually not very large. That is, the required small frequency difference for PRS may have practical applications such as explaining the long connections of brain functional networks, in contrast to the theoretical meaning of the required large frequency difference for RS.

The model in Fig. 1 can also be analyzed from another angle. If we consider all the connected leaf nodes and the hub node as a whole, this combination will be equivalent to a “big hub.” Especially, it is not strange to observe PRS in the indirectly connected leaf nodes when all the nodes in the big hub are synchronized with each other. However, in the model in Fig. 1, the connected leaf nodes are not synchronized with the hub node; thus, they cannot be considered to be a real big hub. Instead, they play a key role in the emergence of PRS among the indirectly connected leaf nodes. Without them, we will not have PRS [see Fig. 2(a)].

On the other hand, the coupling strength  $\alpha\lambda$  in Fig. 1 represents the effect from both the connection between leaf nodes and the influence of other parts of the brain network. In general,  $\alpha$  should be smaller than unity. However, for the nearly identical natural frequencies  $\omega_\ell$  of leaf nodes with small  $\epsilon_\ell$ , two connected leaf nodes can easily be synchronized for smaller  $\alpha$ . In this sense, a further increase in  $\alpha$  will not have more influence on other parts of system. Therefore, the results in Fig. 3 for  $\alpha = 1.0$  and  $0.5$  can also be observed for cases with smaller  $\alpha$ .

In conclusion, we presented a model of a star-like graph to study RS for realistic systems such as brain functional networks. We found that RS can still be observed when we consider only the indirectly connected leaf nodes and called it PRS. We also found the phenomenon of double PRS, except in the single PRS. We showed the phase diagram of both the single and double PRS and found that the frequency difference between the hub and leaf nodes is a key quantity influencing the types of PRS. Further, we showed that more connections

among the leaf nodes favor PRS. A brief theoretical analysis was provided to explain these results. These findings highlight the fundamental question of how the brain functional network emerges from the brain structural network.

## ACKNOWLEDGMENTS

This work was partially supported by STI2030-Major Projects No. 2021ZD0202600 and the NNSF of China under Grants No. 11835003 and No. 12175070.

## APPENDIX A: PARTIAL REMOTE SYNCHRONIZATION IN BRAIN FUNCTIONAL NETWORKS

One of the key problems in neuroscience is to understand how the long connections of brain functional networks come from the short connections of neural networks. So far, a promising way to solve this problem is by RS. However, RS is based on a pure star graph and thus is still a little far away from real brain functional networks. To go forward a substantial step, in this work, we consider the case of a more realistic star-like graph with partial connections among its leaf nodes and discuss its RS. Surprisingly, we find that we cannot observe RS again because the connected leaf nodes are easier to synchronize than those indirectly connected leaf nodes. This finding seems to indicate that RS does not work for realistic brain functional networks, which is not good news for the understanding of how the long connections of brain functional networks come from the short connections of neural networks. Fortunately, we further reveal the phenomenon of PRS and thus extend the concept of RS to realistic situations. In this sense, it will be better if we can provide some evidence to support the concept of PRS, which is the purpose of this Appendix.

To determine the evidence for PRS in realistic situations, we turn to the brain structural network and its corresponding brain functional network. For this purpose, we employ the weighted network of the cerebral cortex from the data of Refs. [34,36], which was partitioned into 989 nodes with  $L = 17\,865$  connections [37]. By checking all 989 nodes and their nearest neighbors, we find that for each node, some of its nearest neighbors are connected to each other while the others are not. Figure 7(a) shows such an example, where the red node represents the hub and the five blue nodes represent the leaf nodes. We see from Fig. 7(a) that there is one connection among the leaf nodes, indicating that it belongs to the motif of the star-like network in Fig. 1.

Then, we consider the corresponding functional network of Fig. 7(a), whose nodes are the same as those of the structural network but whose connections are different; that is, the structural matrix  $\{W_{ij}\}$  is different from the functional matrix  $\{F_{ij}\}$ . For this purpose, we consider the empirical data for the resting-state functional connectivity from Ref. [34]. By focusing on each individual node in Fig. 7(a) and checking the functional connections among its nearest neighbors, we find that some new connections emerge and, at the same time, some old connections disappear, confirming the existence of PRS. As an example, Fig. 7(b) shows the functional connections among the five leaf nodes in Fig. 7(a). Comparing Fig. 7(b) to Fig. 7(a), we see that only one connection between

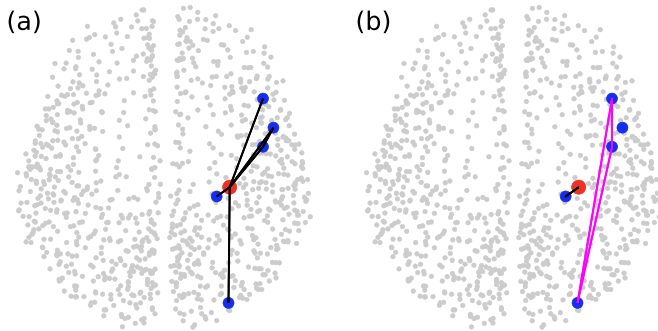


FIG. 7. PRS in a realistic resting-state brain functional network. (a) shows a typical star-like motif from the brain structural network with 989 nodes from the Refs. [34,36], where the red node represents the hub and the five blue nodes represent the leaf nodes. (b) shows the functional connections among the five leaf nodes in (a), where the only black line represents the remaining old connection in (a) and the three pink lines represent the new emerging connections of PRS.

the hub and leaf nodes in Fig. 7(a) remains in Fig. 7(b) (see the black line) and, at the same time, three new connections emerge in Fig. 7(b) (see the three pink lines), indicating that remote synchronization has occurred in the unconnected neighboring nodes of the structural network but not all the neighboring nodes, thus confirming PRS.

### APPENDIX B: PARTIAL REMOTE SYNCHRONIZATION IN CHAOTIC SYSTEMS

To study PRS in chaotic systems, we take the network motif in Fig. 2(d) as an example and consider the nodes as piecewise Rossler units [38]:

$$\begin{aligned} \dot{x}_i &= -\alpha_i \left\{ \Gamma \left[ x_i - \frac{\lambda}{k_i} \sum_{j=1}^5 a_{ij}(x_j - x_i) \right] + \beta y_i + \sigma z_i \right\}, \\ \dot{y}_i &= -\alpha_i(-x_i + v y_i), \\ \dot{z}_i &= -\alpha_i[-g(x_i) + z_i], \end{aligned} \tag{B1}$$

where the piecewise part is  $g(x_i) = 0$  if  $x_i \leq 3$  and  $g(x_i) = \mu(x_i - 3)$  otherwise. The parameters are taken as  $\Gamma = 0.05$ ,  $\beta = 0.5$ ,  $\sigma = 1$ ,  $\mu = 15$ , and  $v = 0.02 - 10/H$ , with

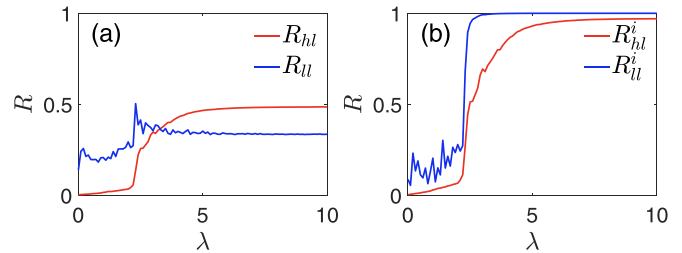


FIG. 8. PRS in a chaotic system of piecewise Rossler units with the network motif from Fig. 2(d). (a) shows the group of all nodes, where the red and blue lines represent the dependence of  $R_{hl}$  and  $R_{ll}$  on the coupling strength  $\lambda$ , respectively. (b) shows the group of indirectly connected leaf nodes, where the red and blue lines represent the dependence of  $R_{hl}^i$  and  $R_{ll}^i$  on the coupling strength  $\lambda$ , respectively.

$H = 55$  being a tunable quantity that regulates the dynamical state of the system.  $A = \{a_{ij}\}$  is the adjacency matrix ( $a_{ij} = 1$  if nodes  $i$  and  $j$  are connected and 0 otherwise),  $\lambda$  is the coupling strength, and  $k_i$  is the degree of the node, with  $k_h = 4$ ,  $k_2 = k_3 = 2$ , and  $k_4 = k_5 = 1$ . The difference between the natural frequencies of the nodes is implemented by letting  $\alpha_h = 3.5$  for the hub node and  $\alpha_\ell$  be randomly chosen from (1.98, 2.02) for all four leaf nodes.

For each node  $i$ , the instantaneous phase at time  $t$  is geometrically evaluated [39] as  $\theta_i = \arctan(y_i/x_i)$ . Then, we calculate the order parameters  $R_{hl}$  and  $R_{ll}$  of all the nodes and the order parameters  $R_{hl}^i$  and  $R_{ll}^i$  of the indirectly connected leaf nodes. Figure 8(a) shows the results for the group of all the nodes, where the red and blue lines represent the dependence of  $R_{hl}$  and  $R_{ll}$  on the coupling strength  $\lambda$ , respectively. We see that with the increase of the coupling strength  $\lambda$ , neither  $R_{hl}$  nor  $R_{ll}$  will reach unity, indicating that there is no synchronization or remote synchronization. However, this conclusion will change when we calculate the quantities of  $R_{hl}^i$  and  $R_{ll}^i$  for the indirectly connected leaf nodes. Figure 8(b) shows the results for the group of indirectly connected leaf nodes, where the red and blue lines represent the dependence of  $R_{hl}^i$  and  $R_{ll}^i$  on the coupling strength  $\lambda$ , respectively. We see that with the increase in  $\lambda$ ,  $R_{ll}^i$  will reach unity for  $\lambda > 2.8$ , while  $R_{hl}^i$  remains less than unity, indicating a typical PRS. Therefore, PRS can be observed in chaotic systems.

[1] Y. Iturria-Medina, A. Pérez Fernández, D. M. Morris, E. J. Canales-Rodríguez, H. A. Haroon, L. García Pentón, M. Augath, L. Galán García, N. Logothetis, G. J. M. Parker, and L. Melie-García, Brain hemispheric structural efficiency and interconnectivity rightward asymmetry in human and nonhuman primates, *Cereb. Cortex* **21**, 56 (2011).  
 [2] Y. Chen, S. Wang, C. C. Hilgetag, and C. Zhou, Trade-off between multiple constraints enables simultaneous formation of modules and hubs in neural systems, *PLoS Comput. Biol.* **9**, e1002937 (2013).  
 [3] Y. Chen, S. Wang, C. C. Hilgetag, and C. Zhou, Features of spatial and functional segregation and integration

of the primate connectome revealed by trade-off between wiring cost and efficiency, *PLoS Comput. Biol.* **13**, e1005776 (2017).  
 [4] L. Cao and Z. Liu, How IQ depends on the running mode of brain network? *Chaos* **30**, 073111 (2020).  
 [5] G. Buzsáki, *Rhythms of the Brain* (Oxford University Press, New York, 2006).  
 [6] F. Varela, J.-P. Lachaux, E. Rodriguez, and J. Martinerie, The brainweb: Phase synchronization and large-scale integration, *Nat. Rev. Neurosci.* **2**, 229 (2001).  
 [7] A. Bergner, M. Frasca, G. Sciuto, A. Buscarino, E. J. Ngamga, L. Fortuna, and J. Kurths, Remote synchronization in star networks, *Phys. Rev. E* **85**, 026208 (2012).



- [8] K. Okuda and Y. Kuramoto, Mutual entrainment between populations of coupled oscillators, *Prog. Theor. Phys.* **86**, 1159 (1991).
- [9] M. Kumar and M. Rosenblum, Two mechanisms of remote synchronization in a chain of Stuart-Landau oscillators, *Phys. Rev. E* **104**, 054202 (2021).
- [10] T. Wu, X. Zhang, and Z. Liu, Understanding the mechanisms of brain functions from the angle of synchronization and complex network, *Front. Phys.* **17**, 31504 (2022).
- [11] Z. Wang and Z. Liu, Partial synchronization in complex networks: Chimera state, remote synchronization, and cluster synchronization, *Acta Phys. Sin.* **69**, 088902 (2020).
- [12] Z. Wang and Z. Liu, A brief review of chimera state in empirical brain networks, *Front. Physiol.* **11**, 724 (2020).
- [13] V. Nicosia, M. Valencia, M. Chavez, A. Diaz-Guilera, and V. Latora, Remote synchronization reveals network symmetries and functional modules, *Phys. Rev. Lett.* **110**, 174102 (2013).
- [14] I. Ruvinsky and J. J. Gibson-Brown, Genetic and developmental bases of serial homology in vertebrate limb evolution, *Development* **127**, 5233 (2000).
- [15] V. Vuksanovic and P. Hovel, Functional connectivity of distant cortical regions: Role of remote synchronization and symmetry in interactions, *NeuroImage* **97**, 1 (2014).
- [16] J. Lacerda, C. Freitas, and E. Macau, Multistable remote synchronization in a star-like network of non-identical oscillators, *Appl. Math. Modell.* **69**, 453 (2019).
- [17] L. Kang, Z. Wang, S. Huo, C. Tian, and Z. Liu, Remote synchronization in human cerebral cortex network with identical oscillators, *Nonlinear Dyn.* **99**, 1577 (2020).
- [18] H. Cao, Z. Yang, and Z. Liu, Remote synchronization in multi-layered community networks with star-like topology, *Chaos Solitons Fractals* **166**, 112893 (2023).
- [19] Z. Yang, D. Chen, Q. Xiao, and Z. Liu, Phase frustration induced remote synchronization, *Chaos* **32**, 103125 (2022).
- [20] H. Sakaguchi and Y. Kuramoto, A soluble active rotator model showing phase transitions via mutual entrainment, *Prog. Theor. Phys.* **76**, 576 (1986).
- [21] G. Rosell-Tarrago and A. Diaz-Guilera, Functionability in complex networks: Leading nodes for the transition from structural to functional networks through remote asynchronization, *Chaos* **30**, 013105 (2020).
- [22] S. Lee and K. Krischer, Attracting Poisson chimeras in two-population networks, *Chaos* **31**, 113101 (2021).
- [23] J. Fell and N. Axmacher, The role of phase synchronization in memory processes, *Nat. Rev. Neurosci.* **12**, 105 (2011).
- [24] S. Majhi, B. K. Bera, D. Ghosh, and M. Perc, Chimera states in neuronal networks: A review, *Phys. Life Rev.* **28**, 100 (2019).
- [25] S. Boccaletti, J. Kurths, G. Osipov, D. L. Valladares, and C. S. Zhou, The synchronization of chaotic systems, *Phys. Rep.* **366**, 1 (2002).
- [26] A. Pikovsky, M. Rosenblum, and J. Kurths, *Synchronization: A Universal Concept in Nonlinear Sciences* (Cambridge University Press, Cambridge, 2001).
- [27] A. Maritan and J. R. Banavar, Chaos, noise, and synchronization, *Phys. Rev. Lett.* **72**, 1451 (1994).
- [28] D. S. Goldobin and A. Pikovsky, Synchronization and desynchronization of self-sustained oscillators by common noise, *Phys. Rev. E* **71**, 045201(R) (2005).
- [29] T. Wu, S. Huo, K. Alfaro-Bittner, S. Boccaletti, and Z. Liu, Double explosive transition in the synchronization of multilayer networks, *Phys. Rev. Res.* **4**, 033009 (2022).
- [30] M. A. Kramer and S. S. Cash, Epilepsy as a disorder of cortical network organization, *Neuroscientist* **18**, 360 (2012).
- [31] Q. Shen and Z. Liu, Echo effect in brain networks, *Chaos Solitons Fractals* **160**, 112260 (2022).
- [32] A. Shoeb, Application of machine learning to epileptic seizure onset detection and treatment, Ph.D. thesis, Massachusetts Institute of Technology, 2009; CHB-MIT Scalp EEG Database, <https://physionet.org/content/chbmit/1.0.0/>.
- [33] M. Torkamani-Azar, S. D. Kanik, S. Aydin, and M. Cetin, Prediction of reaction time and vigilance variability from spatio-spectral features of resting-state EEG in a long sustained attention task, *IEEE J. Biomed. Health Inf.* **24**, 2550 (2020); SPIS-Resting-State-Dataset, <https://github.com/mastaneht/SPIS-Resting-State-Dataset>.
- [34] C. J. Honey, O. Sporns, L. Cammoun, X. Gigandet, J. P. Thiran, R. Meuli, and P. Hagmann Predicting human resting-state functional connectivity from structural connectivity, *Proc. Natl. Acad. Sci. USA* **106**, 2035 (2009).
- [35] S. Huo and Z. Liu, Condensation of eigenmodes in functional brain network and its correlation to chimera state, *Commun. Phys.* **6**, 285 (2023).
- [36] P. Hagmann, L. Cammoun, X. Gigandet, R. Meuli, C. J. Honey, V. J. Wedeen, and O. Sporns, Mapping the structural core of human cerebral cortex, *PLoS Biol.* **6**, e159 (2008).
- [37] S. Huo, C. Tian, M. Zheng, S. Guan, C. Zhou, and Z. Liu, Spatial multi-scaled chimera states of cerebral cortex network and its inherent structure-dynamics relationship in human brain, *Natl. Sci. Rev.* **8**, nwaal25 (2021).
- [38] I. Leyva, R. Sevilla-Escoboza, J. M. Buldú, I. Sendiña-Nadal, J. Gómez-Gardeñes, A. Arenas, Y. Moreno, S. Gómez, R. Jaimes-Reátegui, and S. Boccaletti, Explosive first-order transition to synchrony in networked chaotic oscillators, *Phys. Rev. Lett.* **108**, 168702 (2012).
- [39] G. V. Osipov, A. S. Pikovsky, M. G. Rosenblum, and J. Kurths, Phase synchronization effects in a lattice of nonidentical Rossler oscillators, *Phys. Rev. E* **55**, 2353 (1997).